J. Micromech. Microeng. 6 (1996) 337–344. Printed in the UK

An energy-based design criterion for magnetic microactuators

Z Nami†, C H Ahn‡ and M G Allen†

† Microelectronics Research Center, School of Electrical and Computer Engineering, Georgia Institute of Technology, Atlanta, GA 30322-0269, USA
‡ Center for Microelectronic Sensors and MEMS, Department of Electrical and Computer Engineering and Computer Science, University of Cincinnati, Cincinnati, OH 45221-0030, USA

Received 29 April 1996, accepted for publication 24 June 1996

Abstract. Magnetic actuators can be divided into two types: those in which motion changes the gap separation (type I) and those in which motion changes the gap overlap area but not the gap separation (type II). In conventional magnetic actuators of both types, it is assumed that most of the magnetic energy is stored in the gap due to the large reluctance of the gap compared with the negligibly small reluctance of the magnetic core. However, in magnetic microactuators, the fabrication limitations on the achievable cross-sectional area of the magnetic core as well as the finite core permeability increase the core reluctance to the point that this assumption may no longer be valid. In this case, the magnetic energy is distributed in both the gap and the magnetic core, in which the energy distribution is in proportion to the reluctance of the gap (R_{gap}) and the reluctance of the core (R_{core}) respectively. Using an elementary structure of a magnetic actuator, it is shown that for type I microactuators, when the initial gap of the actuator is fixed (e.g., determining the stroke of the actuator), the generated magnetic force has maximum value when the gap overlap area is designed such that the reluctance of the gap is equal to the reluctance of the magnetic core (i.e., $R_{gap} = R_{core}$). For type II actuators, the initial overlap area of the actuator is fixed (determining the stroke); therefore the generated magnetic force has a maximum value when the gap separation is designed such that the above equality holds. This paper details both analytical and finite element method (FEM) analysis confirmation for type I actuators. Extension to type II actuators is straightforward.

1. Introduction

Macro-scale magnetic actuators have been widely used in applications ranging from motors to magnetic relays. Many design criteria and analysis methods have been developed to predict and to analyse their performance. Recently, micromachined versions of these magnetic actuators have become available [1–8]. However, in analysing these magnetic microactuators, it is apparent that some of the assumptions which are perfectly adequate for macro-scale actuators are unacceptable in the micro-scale. The purpose of this paper is to describe which of these assumptions are not valid and why, and to show that in certain cases, the use of intuition and design criteria which are appropriate in the macro-scale is inappropriate on the micro-scale.

In the conventional analysis of the macro-scale magnetic actuator, most of the magnetic energy is stored in the gap included in the magnetic circuit due to the large reluctance of the gap compared with the negligibly small reluctance of the core. However, in analysing magnetic microactuators, the assumption of gap reluctance dominance may not be acceptable in the micro-scale. In magnetic microactuators, the reluctance of the magnetic core has a comparable value to or even exceeds that of the gap. In these reluctance-limited actuators, magnetic energy is distributed in both the gap and the magnetic core. By using a model structure of a magnetic actuator, it can be shown that the stored magnetic energy and the magnetic force generated in the gap have a maximum value when both reluctances of the gap and core are equal. This condition would be an appropriate 'rule of thumb' in the design of magnetic microactuators for maximum force.

In general, two different types of actuators, denoted type I and type II, can be realized (see figure 1). In the type I actuator, the displacement due to the magnetic force applied to the movable part of the actuator is in the direction of the gap separation. The initial gap separation in this case is determined by the desired actuator stroke. In this case, for maximum force, the gap area can be designed for reluctance equivalence. In the type II actuator, the displacement due to the magnetic force is normal to the direction of the gap separation. For this type of actuator, the initial gap area is fixed by the actuator stroke and it is the gap separation that can be adjusted according to the design criterion. Since the result of reluctance equivalence holds for both types of actuators, it is necessary to examine in

0960-1317/96/030337+08$19.50

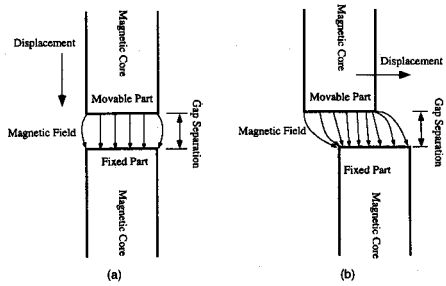

Figure 1. Schematic diagram of the two different types of magnetic microactuators as defined in this paper. (a) type I microactuator; (b) type II microactuator.

detail only one actuator type. In this paper, both analytical modeling and finite element (FEM) analysis of type I actuators are examined. Extrapolation of these results to type II actuators is straightforward.

2. Magnetic circuit analysis

Before performing magnetic circuit analysis on a given actuator, if a scaling boundary between the macro-scale and the micro-scale could be defined, it would be convenient in determining whether conventional or reluctance-limited analyses are required. Unfortunately, no strict size-based rules exist to define the boundary between these analyses. Although the selection of analysis cannot be determined based solely on geometrical size, it can be done based on relative core and gap reluctance values. For magnetic microactuators, core reluctances often increase to non-negligible values compared to gap reluctances due both to limitations on core thickness and achievable material permeability. For these reasons, magnetic microactuators commonly fall into the reluctance-limited or micro-scale analysis.

2.1. Conventional (macro-scale) analysis

For the macro-scale analysis, consider the type I magnetic actuator shown in figure 2. The core is made of a magnetic material with a permeability μ and has constant cross-sectional area A_c. The gap, of area A_g and separation g, is shown on the structure. The total length of the core and the overlap length are denoted by ℓ_c and ℓ_{ol}, respectively.

In figure 2, neglecting fringing, the magnetic reluctance of the gap (R_{gap}) and of the magnetic core (R_{core}) are as follows

$$R_{gap}(x) = \frac{(g-x)}{\mu_0 A_g} \tag{1}$$

$$R_{core} = \frac{\ell_c}{\mu A_c} \tag{2}$$

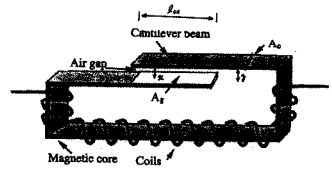

Figure 2. Schematic diagram of a magnetic actuator.

where g is the initial gap separation before a motion takes place and x is the extent of motion normal to the surface of the gap electrode. It is assumed that the actuator motion does not alter the core reluctance. To consider the initial force on the actuator (i.e., the force prior to motion), x can be taken equal to zero.

In this conventional case, the reluctance of the magnetic core is usually negligibly small compared with that of the gap; thus it is assumed that most of the magnetic energy is stored in the gap. As the moving part is displaced due to the generated mechanical force at the gap, the inductance of the excitation coil varies as a function of position of the moving part due to the reluctance variation of the gap.

For a linear system, the energy and co-energy are numerically equal. Therefore, the inductance (L), magnetic stored energy (W_m), and magnitude of the mechanical force in the x-direction (F_x) on the structure can be shown as [9]:

$$L(x) = \frac{N^2}{R_{gap}(x)} \tag{3a}$$

$$W_m = \frac{1}{2} i^2 L(x) \tag{3b}$$

$$F_x = \frac{\partial W_m}{\partial x} = \frac{A_g}{2\mu_0}\left(\frac{iN\mu_o}{g-x}\right)^2 \tag{3c}$$

where N is the number of coil turns and i is the excitation current. Note that it is assumed that the reluctance of the magnetic core is negligibly small. As equation (3c) shows, the generated force increases as the actuation motion decreases the gap separation. Thus, in order to exert a maximum force in the actuator, the gap should be made as small as possible and the overlap area made as large as possible since the force increases monotonically as the gap separation shrinks and the gap area increases.

2.2. Reluctance-limited (micro-scale) analysis

For the purposes of this analysis, the assumption of negligible core reluctance is relaxed. In addition, it is assumed that the magnetic material is magnetically linear. The same approach described in the previous section to analyse the actuator shown in figure 2 is used. Since the ratio of energy stored in the gap to that in the core is in proportion to the reluctances of the gap and the core, these energies are derived as

$$W_{core} = \frac{1}{2}\frac{N^2i^2R_{core}}{(R_{core}+R_{gap})^2} \tag{4}$$

$$W_{gap} = \frac{1}{2}\frac{N^2i^2R_{gap}}{(R_{core}+R_{gap})^2}. \tag{5}$$

The total energy stored in the system is the sum of the energy stored in the core and in the gap. It is determined from the above equations as

$$W_m = \frac{1}{2}i^2L(x) = W_{core} + W_{gap} = \frac{1}{2}\frac{N^2i^2}{(R_{core}+R_{gap})}. \tag{6}$$

The magnitude of the force of magnetic origin acting to close the gap is the derivative of equation (6) with respect to the gap variation:

$$F_x = \frac{\partial W_m}{\partial x} = \frac{1}{2}\frac{N^2i^2}{\mu_0 A_g (R_{gap}+R_{core})^2} \tag{7}$$

and the substitution of equations (1) and (2) into equation (7) gives

$$F_x = \frac{1}{2}\frac{N^2i^2}{\mu_0 A_g\left(\frac{l_c}{\mu A_c}+\frac{g-x}{\mu_0 A_g}\right)^2}. \tag{8}$$

Note that equation (8) is the same expression as equation (3c), except that the core reluctance is no longer neglected.

In the conventional analysis, equation (3c) shows that the smaller the gap separation and the larger the gap overlap area that is achieved, the larger the generated force, which can be considered as a design criterion for conventional magnetic actuators. The corresponding design criterion from equation (8) for the micro-scale (i.e., when core reluctance can no longer be neglected) can be determined by differentiating equations (5) or (8) with respect to appropriate geometrical variables, to test whether or not the stored gap energy or the generated magnetic force has a maximum value at a given gap geometry.

In the type I microactuator (i.e., where actuation changes gap separation), there are two ways to adjust the reluctance in the magnetic core (R_{core}) for a given permeability: the core cross-sectional area A_c and the core length ℓ_c. The variation of the core cross-sectional area in a planar-type integrated inductive component [10–12] is limited by the achievable thickness as well as the width of the core, as magnetic microdevices are usually implemented in a planar fashion. The core length ℓ_c is mainly determined by the required number of coil turns necessary to attain a required magnetic flux density in the device. Consequently, the adjustment of the geometrical dimension to vary the magnetic core reluctance is usually limited.

However, the geometrical variables for the gap reluctance (R_{gap}) can be flexibly adjusted by varying the gap area A_g (or the overlapped length ℓ_{ol}) and the initial gap g. In a type I actuator, the initial gap is usually set by the desired range of actuation. In addition, for the microactuator shown in figure 2, the maximum achievable gap separation is limited due to the limitation of the thickness of deposited sacrificial layers. However, the gap area A_g (or the overlap length ℓ_{ol}) can be easily adjusted by varying either the overlap gap width or length. Thus, by differentiating equation (5) with respect to the gap area A_g and then by equating it to zero, it is found that the energy stored in the gap has a maximum value when

$$R_{gap} = R_{core}. \tag{9}$$

This also can be verified by differentiating equation (8) with respect to the gap area A_g and then by equating to zero. The condition described in equation (9) can serve as the criterion for maximum force in designing magnetic microactuators in the micro-scale. It is interesting to note that the condition implied in equation (9) is analogous to the maximum power-transfer condition in an electrical circuit to transfer a maximum power to a load (R_l) from a power source which includes an internal source resistance (R_s), where the condition is $R_l = R_s$.

Thus, when the reluctance of the core cannot be neglected, careful sizing of the gap area and/or the initial gap separation are necessary to satisfy the maximum force design criterion of magnetic microactuators. In the next section, magnetic microactuators which are realized in this 'core-limited' regime will be analysed.

3. Magnetic microactuator analysis

In applying the design criterion defined in equation (9), a type I magnetic microactuator with a nickel/iron cantilever beam [5–6] will be considered. As mentioned above, a type I microactuator has a gap geometry such that the gap separation $(g - x)$ is varied during actuation, but the gap area is constant. Consequently, in designing this actuator, one design methodology would be to size the gap by the deflection range requirement, then adjust the gap area to satisfy equation (9).

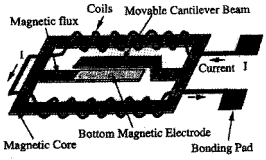

Figure 3. Schematic diagram of planar magnetic microactuator with a cantilever beam.

3.1. Analytical modeling

In this section, the maximum force criterion is applied to the analysis of a realized deflecting magnetic microactuator. Figure 3 shows the microactuator to be analysed.

The magnetic flux that crosses a gap in the magnetic circuit produces an attractive force between the faces of the magnetic electrodes. The magnetic core structure contains a gap with a variable length $(g - x)$ which is determined by the position of the movable cantilever beam. In this analytical modeling, the fringing effect is neglected.

The paths of magnetic flux in the actuator under discussion are shown in figure 4(a). Magnetic analysis can be facilitated by introducing the equivalent electrical circuit of figure 4(b), in which the resistances, R_0 and R_1 indicate the magnetic reluctance, and the voltage source F denotes the magnetomotive force (mmf). This circuit can be simplified in figure 4(c) if the reluctance R_{core} is given by

$$R_{core} = \frac{R_1}{2} + R_0 = \frac{(0.5l_{c1} + l_{c0})}{\mu A_c} \tag{10}$$

From equations (4)–(6), the total magnetic energy (W_m) as well as the gap energy (W_{gap}) and the core energy (W_{core}) can then be expressed as

$$W_m = \frac{1}{2}\frac{i^2 N_1^2 \mu_0 \mu A_c A_g}{0.5\mu_0 l_{c1} A_g + \mu_0 l_{c0} A_g + \mu A_c (g - x)} \tag{11a}$$

$$W_{gap} = \frac{1}{2}\frac{i^2 N_1^2 \left(\frac{g-x}{\mu_0 A_g}\right)}{\left[\frac{(0.5l_{c1}+l_{c0})}{\mu A_c} + \frac{g-x}{\mu_0 A_g}\right]^2} \tag{11b}$$

$$W_{core} = \frac{1}{2}\frac{i^2 N_1^2 \left(\frac{(0.5l_{c1}+l_{c0})}{\mu A_c}\right)}{\left[\frac{(0.5l_{c1}+l_{c0})}{\mu A_c} + \frac{g-x}{\mu_0 A_g}\right]^2} \tag{11c}$$

where N_1 is the number of coil turns in l_{c1}, A_c is the cross-sectional area of magnetic core in the inductive component, and g is the initial gap spacing.

From equation (7), the generated magnetic force on the deflecting cantilever beam is

$$F_x = \frac{A_g}{2\mu_0}\left(\frac{i^2 N_1^2 \mu_0 \mu A_c}{0.5\mu_0 l_{c1} A_g + \mu_0 l_{c0} A_g + \mu A_c (g - x)}\right)^2. \tag{12}$$

The magnetic energy stored in the magnetic core and gap and the total stored energy for the fabricated magnetic microactuator can be calculated from equations (11*a*)–(11*c*). To calculate the magnetic energy stored in the magnetic core and gap shown in figure 4(c), the geometrical and magnetic parameters of the magnetic microactuator are used as follows: $N_1 i = 0.5$ ampere-turns, $t = 12$ μm, $A_c = w \cdot t$, $A_g = w \cdot \ell_{ol}$, $w = 1$ cm, $g = 10$ μm, $\mu = 5000\mu_0$, total core length $(0.5l_{c1} + l_{c0})$ of 3478 μm, and ℓ_{ol} denotes the overlap length of cantilever beam. Equations (11) and (12) yield the stored energy and the magnitude of the x-directed force over the deflection range of the actuator. For comparison purposes, it is convenient to consider the energy and force at one actuator position so that the effect of geometry on the energy and force can plainly be seen. This can be accomplished by evaluating equations (11*b*) and (12) at $x = 0$ (the undeflected state). Figure 5 shows a plot of these two equations as a function of the overlapped length ℓ_{ol} for the actuator in the undeflected state. Both gap energy and force can be seen to have a maximum value at an overlap length of approximately 175 μm. This overlap length (gap area) also satisfies the design criterion defined in equation (9).

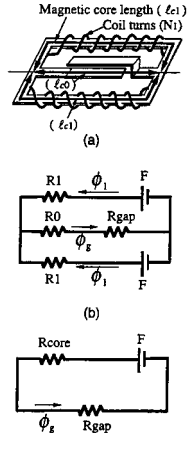

Figure 4. Magnetic circuit model of the microactuator and the analogous equivalent electrical circuit. (a) actuator with defined parameters; (b) equivalent electrical circuit, where R_0, R_1 and R_{gap} are the reluctances corresponding to the magnetic circuit branches and gap respectively. F denotes the corresponding magnetomotive force; (c) simplified circuit.

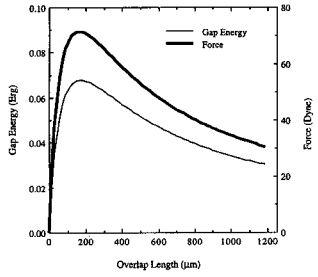

Figure 5. Magnetic energy stored and magnetic force generated in the gap as a function of the overlap length of the cantilever beam, where both maxima occur at an overlap length of 175 μm (which satisfies the condition of $R_{gap} = R_{core}$).

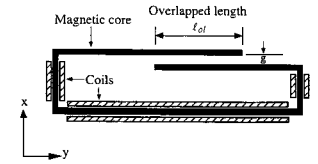

Figure 6. Simplified model of magnetic microactuator from figure 3 for FEM analysis.

3.2. Finite element method (FEM) analysis

To verify the design criterion by FEM analysis, the simplified structure shown in figure 6 (i.e., the structure corresponding to the simplified magnetic equivalent circuit shown in figure 4(c)), was modeled. Once the magnetic potential has been determined by FEM to appropriate numerical accuracy, the magnetic flux density, B, is obtained numerically by taking the curl of the vector potential field. The energy stored in the volume described by each element can then be determined from the equation

$$W_{elem} = \frac{B_{elem}^2}{2\mu_{elem}} V_{elem}. \tag{13}$$

As some of the elements denote non-magnetic environment (e.g., air), and some of the elements denote core material, the energies in the air and the core can be independently determined by adding up the contributions from air elements and core elements. The total stored energy can then be determined by adding these two energies.

In order to calculate the force, a numerical approximation of equation (7) is used. For example, to calculate the force in the x-direction, two finite element simulations are run; one with the cantilever beam position at x, and one with the cantilever beam position at $x + \Delta x$. The two total energies, $W(x)$ and $W(x + \Delta x)$ are then calculated. The magnitude of the force in the x-direction of the actuator in its undeflected state is then determined as

$$F_x = \frac{W(x + \Delta x) - W(x)}{\Delta x}. \tag{14}$$

The magnitude of the force in the y-direction can be determined by a similar procedure.

A magnetic material with a $\mu = 5000\mu_0$ is also assumed. In figure 6, the total core length is 3478 μm, its width t is 12 μm, and its initial gap g is 10 μm. The overlap length (i.e., gap area and therefore gap reluctance) ℓ_{ol} between the top cantilever beam and bottom magnetic core is varied as a simulation parameter.

This simplified magnetic microactuator is modeled using the magnetic analysis of the computer program ANSYS [14]. The flux density distributions both in the gap and in the magnetic core are shown in figure 7(a) and (b) respectively for a 780 μm overlap length, where different shading indicates different flux density (Gauss) distributions. In figure 7, CGS units are used due to the small dimensions of the microactuator and the analysed structure is not drawn to scale (the x-direction expanded by a factor of 7) to specifically show the magnetic flux density distribution around the gap. The magnetic flux is not completely confined inside of the gap but flows through the surrounding air outside of the end-tips of cantilever beam, which indicates that the cantilever beam gap has magnetic fringing at the tips. The magnetic flux density is not distributed uniformly through the gap area, and thus several times higher magnetic flux density is achieved at the tip of the cantilever beam compared with that of the center, depending on the variation of the overlap length.

The stored energy in the magnetic core and the gap, as well as the resultant forces on the cantilever beam, are obtained using the methods described above as a function of overlap length (gap reluctance). From the FEM analysis, the magnetic energies which are stored in the magnetic core and the gap as a function of overlap length are plotted in figure 8.

In figure 9, magnetic energies in the gap as determined by both FEM and analytical calculation are shown. From the FEM analysis, the functional form of the analytical analysis is confirmed. However, the magnetic energy stored in the gap from FEM analysis is larger than the result from the analytical evaluation due to fringing. Also the maximum energy in the gap occurs at an overlap of 140 μm which is shorter than that of the analytical result (175 μm). This shorter overlap can again be explained by the magnetic fringing as shown in figure 7. In other words, the 'effective' gap overlap area is larger than the actual gap overlap area, since substantial flux is present in the air outside the gap. In this fringing-influenced case, the maximum gap energy is achieved where the effective gap and core reluctances are equal. The overlap difference of 35 μm between the analytical and the FEM solutions can be used to evaluate the magnitude of the fringing effect in this microactuator.

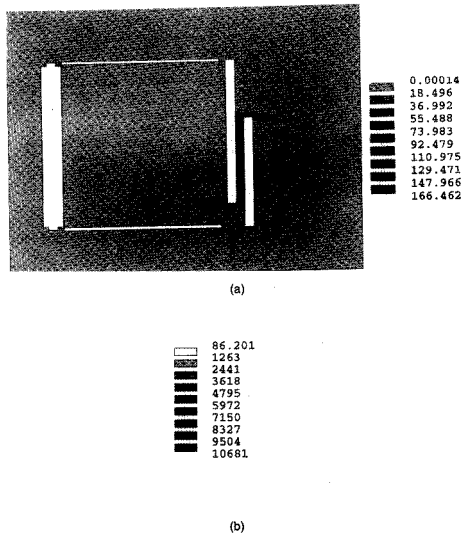

Figure 7. Magnetic flux density (Gauss) distribution obtained from FEM analysis (not to scale): (a) in the gap; (b) in the magnetic core. Different shading corresponds to different densities as shown in the figure.

The evaluated forces from the FEM analysis are shown in figure 10. It is found that there is a peak in the force in the x-direction at the point where the energies of the magnetic core and the air have an equal value. The equality of energies stored in the core and gap leading to maximum force is therefore verified even in the case of fringing, as long as the fringing is small enough that such an equality exists [15]. Note that for small overlaps, the force in the y-direction actually exceeds the force in the x-direction. In this case, if the beam compliance is equal in both directions, the beam could move in the y-direction in addition to bending downward. For larger overlaps, the force in the x-direction is much larger and the cantilever beam bends downward. Both of these cases have also been experimentally observed. The FEM-calculated force in the x-direction matches well with the force calculated analytically as shown in figure 11, except that the exact value of overlap for maximum force is slightly shifted due to fringing.

It is clear that the actuator depicted in figure 3 is a three-dimensional structure which will have fringing in all directions, as opposed to the fringing results predicted by the two-dimensional finite element analysis presented in this paper. Since fringing reduces the required overlap length for reluctance equivalence, it is expected that the overlap length for maximum force will be even smaller than that predicted by the two- dimensional FEM model. Nevertheless, it is clear that by reducing the fringing, either by using higher permeability materials for the magnetic core or by changing the actuator geometry, these differences will be minimized and the simple analytical approach will be adequate.

4. Summary

In this paper, a design criterion for magnetic microactuators has been shown. Due to fabrication constraints, microactuators often operate in the reluctance limited regime. In this regime, maximum energies and forces are found when the actuator is designed such that the gap and core reluctances are equal. For a type I microactuator, in which actuation occurs in the direction of the gap separation, a feasible design sequence would be to size the initial gap separation in accordance with the actuator

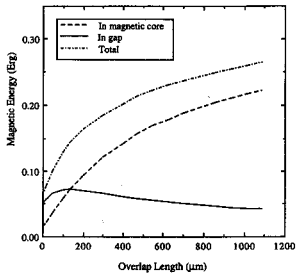

Figure 8. Magnetic energy stored in the gap and the magnetic core by FEM analysis, where the maximum magnetic energy stored in the gap is achieved at 140 μm of overlap length. The total magnetic energy is the sum of gap and core energies.

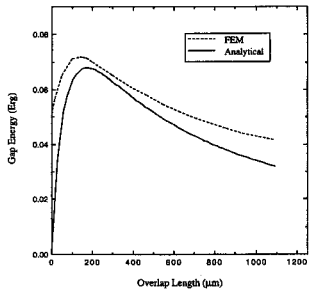

Figure 9. Difference in gap magnetic energy between analytical and FEM analyses.

stroke requirements, then size the gap area such that the reluctances of gap and core are equal. For a type II microactuator, in which actuation changes the gap area but not the gap separation, a feasible design sequence would be to size the initial gap area in accordance with the actuator stroke requirements, then size the gap separation such that the reluctances of gap and core are equal. The analytical result has been verified using finite elements for a previously-developed type I magnetic microactuator. Using finite elements, it is observed that fringing acts to increase the effective gap overlap area, thus decreasing the physical overlap necessary to achieve reluctance equivalence.

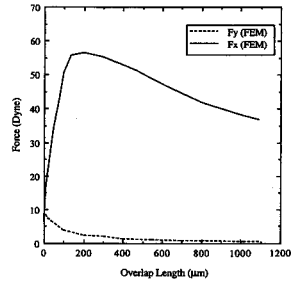

Figure 10. Magnetic force by FEM analysis in x and y directions.

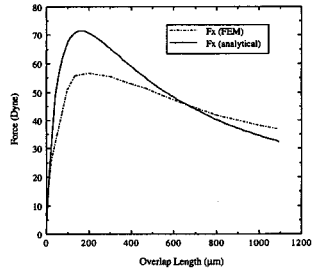

Figure 11. Comparison of magnetic forces in x-direction obtained from both analytical and FEM analyses.

Acknowledgment

This work was supported in part by the National Science Foundation under grant ECS-9117074. The authors would like to thank Mr Yong J Kim at Georgia Tech for valuable technical discussions during the course of this work.

References

[1] Yanagisawa K, Tago A, Ohkubo T and Kuwano H 1991 *Proc. IEEE Microelectromechanical Systems Workshop* pp 120–4

[2] Christenson T R, Guckel H, Skrobis K J and Klein J 1992 *Tech. Digest, IEEE Solid-State Sensor and Actuator Workshop* pp 6–9

[3] Wagner B, Kreutzer M and Benecke W 1992 *Proc. IEEE Microelectromechanical Systems Workshop* pp 183–9

[4] Busch-Vishniac I Jn 1992 The case for magnetically driven microactuators *Sensors Actuators* **A33** 207–20
[5] Ahn C H and Allen M G 1993 *IEEE/ASME J. Microelectromech. Sys.* **2** 15–22
[6] Ahn C H, Kim Y J and Allen M G 1993 *IEEE/ASME J. Microelectromech. Sys.* **2** 165–73
[7] Liu C, Tsao T, Tai Y C and Ho C M 1994 *Proc. IEEE Microelectromechanical Systems Workshop* pp 57–62
[8] Judy J W, Muller R S and Zappe H H 1994 *Solid-State Sensor and Actuator Workshop* pp 43–8
[9] White D C and Woodson H H 1959 *Electromechanical Energy Conversion* (New York: Wiley)
[10] Oshiro O, Tsujimoto H and Shirae K 1987 A novel miniature planar inductor *IEEE Trans. Magnetics* **MAG-23** 3759–61
[11] Ahn C H and Allen M G 1994 *IEEE Trans. Magnetics* **31** 73–9
[12] Ahn C H, Kim Y J and Allen M G 1993 *Transducers, 7th Int. Conf. on Solid-State Sensors and Actuators* pp 70–3
[13] Silvester P P and Ferrari R L 1983 *Finite Elements For Electrical Engineers,* (Cambridge: Cambridge University Press)
[14] Kohnke P C 1987 *ANSYS Theoretical Manual* Swanson Analysis Systems, Inc., Houston, PA
[15] Nami Z, Ahn C H and Allen M G 1993 *Proc. ASME Winter Annual Meeting, DSC* vol 46, pp 1–6